EDITORS' CHOICE

# Stability of Unstable Perovskites: Recent Strategies for Making Stable Perovskite Solar Cells

Sawanta S. Mali,[1,z] Jyoti V. Patil,[1] Hamidreza Arandiyan,[2] Rafael Luque,[3] and Chang Kook Hong[1,z]

[1]Polymer Energy Materials Laboratory, School of Applied Chemical Engineering, Chonnam National University, Gwangju 500-757, South Korea
[2]Laboratory of Advanced Catalysis for Sustainability, School of Chemistry, The University of Sydney, Sydney 2006, Australia
[3]Departamento de Química Orgánica, Universidad de Córdoba, E14014, Córdoba, Spain

Perovskite solar cells (PSCs) are now crossing the certified 23.2% power conversion efficiency (PCE), however, the stability of organic-lead halide perovskites, cost of additives doped hole transport layer (HTL) and upscaling from lab-scale to industrial scale without hampering its efficiency are challenging tasks for its commercial application. These problems could be tackled via different aspects which includes the synthesis of promising electron transport layers (ETLs) and HTLs, synthesis of mixed perovskites via combination of 3D and stable 2D perovskite, replacement of poor-stable methylammonium (MA) cation with MA free perovskite and capping inorganic materials will be the best choice toward highly efficient air-thermal-stable perovskite solar cells (PSCs). This perspective focuses on the current strategies in PSCs for making the stable PSCs via low-cost, easily processed components and shared our views toward commercialization.

 [DOI: 10.1149/2.0201906jss]

Manuscript submitted April 12, 2019; revised manuscript received June 4, 2019. Published June 18, 2019.

Till-date, the crystalline silicon (c-Si) technology dominate the photovoltaics market due to its 29.4% Auger efficiency limit and continuous efficiency improvement.[1,2] Recently 27.7% power conversion efficiency (PCE) has been reported for the single junction silicon solar cells.[3] Although, dual or multi-junction with III–V materials with c-Si now crossing 32.8% PCE, the expensive deposition methods and tedious procedure hampers the low-cost efficient photovoltaics.[4] Besides, certified PCE of 27.3% (on 1cm$^2$ by Oxford PV)[5] and 25.2% (on 1.419 cm$^2$ by EPFL)[6] have been recently reported based on monolithic perovskite/silicon tandem. However, still Si-based photovoltaics suffered from high-cost and toxic silicon photovoltaic technology.[7,8] After the first demonstration with 3.8% PCE in 2009, perovskite solar cells (PSCs) now crossing >23.3% PCE, competing for the commercial single or multi-junction photovoltaics. Therefore, due to promising materials properties, low-cost and bombing efficiency within a concise period, the PSC is game-changing material in photovoltaic technology.[9–12] Tunable band-gap, a sharp optical absorption edge and simple deposition method are the key properties of lead-halide based PSCs, which makes them to approach 25% PCE at low-cost.

However, long-term stability and upscaling are the main challenges in perovskite photovoltaics. So far, different approaches have been studied by perovskite researchers which includes, deposition methods, perovskite composition, stability, and development of hole-transport layer (HTL), electron transport layer (ETL) and so on. In this perspective, we discussed the current trends in single-junction perovskite photovoltaics, its types, remedies for unstable perovskites and challenges for upscaling.

***Device architecture and role of ETLs and HTLs.—***The ETL, perovskites layer and HTL are the key components of PSCs. The single-junction perovskite solar cells categories in to three different types includes mesoscopic normal (n-i-p), inverted (p-i-n) and HTL free mesoscopic structure.[13] Variety of organic-lead halides has been synthesized and demonstrated its photovoltaic performance which reflects from four-digit publications in each year. However, the mixed-halide mixed-cation based perovskites with modified deposition route such as solvent engineering route holds the peaks efficiency. Basically, perovskite has $AMX_3$ general chemical formula, here M stands for metallic cations and X stands for anions form $MX_6^{4-}$ octahedra with A cations occupying the 12-fold coordinated holes within the cavity. The controlled band bap of a mixed halide-mixed cation $(FAPbI_3)_{0.95}$ $(MAPbBr_3)_{0.05}$ (herein $MAPbBr_3$ stands for methylammonium lead bromide, and $FAPbI_3$ stands for formamidinium lead iodide) processed by solvent engineering method with the reduced trap concentration of bulk perovskite film and precise additives doped novel HTL now crossing 23.2% certified PCE.[14] Newly developed ($N^2$,$N^2$,$N^7$,$N^7$-tetrakis (9,9-dimethyl-9H-fluoren-2-yl)-$N^2$,$N^{2'}$,$N^7$,$N^{7'}$-tetrakis(4-methoxyphenyl)-9,9′ -spirobi [fluorene]-2,2′,7,7′ -tetraamine) (known as DM) showed >23.2% with 120 hours stability at 85°C, with precise doping of 4-tertbutylpyridine (TBP) and bis(trifluoromethane)sulfonimide lithium salt (LiTFSI) additives.

The electron mobility of the $TiO_2$ ETLs has been improved with various dopant, but implementation of chemically processed $BaSnO_3$ nanoparticles of n-type 3.2 eV wide bandgap and its unusual high-electric mobility (320 cm$^2$V$^{-2}$s$^{-1}$) tuned via lanthanum (La) doping which exhibited cubic oxide perovskite structure (Fig. 1A) shows promising efficiency.[15] The fabricated perovskite device based on oxide perovskite La-$BaSnO_3$ ETL, $MAPbI_3$ halide perovskite and poly [bis(4-phenyl)(2,4,6-trimethylphenyl)amine] (PTAA) HTL (Fig. 1B) exhibited an open-circuit voltage (Voc) of 1.12 V, a short-circuit current density (Jsc) of 23.4 mAcm$^{-2}$, and a fill factor (FF) of 81.3%, yielded PCE of 21.3% (Fig. 1C). Here, the conventional HTMs such as $N^2$,$N^2$,$N^{2'}$ $N^{2'}$ $N^7$,$N^7$,$N^{7'}$·$N^{7'}$-octakis(4-methoxyphenyl)-9,9′-spirobi[9H-fluorene]-2,2′,7,7′-tetramine (spiro-OMeTAD) or PTAA are inappropriate for long-term stability due to these organic HTMs can degrade the device performance by morphological deformation, contact metal diffusion and additives. Therefore, inorganic p-type metal oxides such as NiOx has been used and fabricated a two-sided glass-encapsulated architecture by lamination of two half cells (glass/FTO/n-type oxide/$MAPbI_3$ and $MAPbI_3$/NiO/FTO/glass) to form glass/FTO/n-type oxide/$MAPbI_3$/p-type NiO/FTO/glass device architecture. These glass-encapsulated perovskite device architecture retain ~93.3% original efficiency even after 1000 hours (Fig. 1D).

***Role of 2D and 3D composition toward stable carbon-PSCs (C-PSCs).—***Although, mixed halide-mixed cation based PSCs now exceeding >23.2% and >25.2% PCE respectively for single junction and for textured monolithic perovskite/silicon tandem[14–20] through different compositions of MAPbX/FAPbX and mixing of variety of cations such as RbI, CsI and using different HTLs, but still suffered air-

zE-mail: sawantasolar@gmail.com; hongck@chonnam.ac.kr

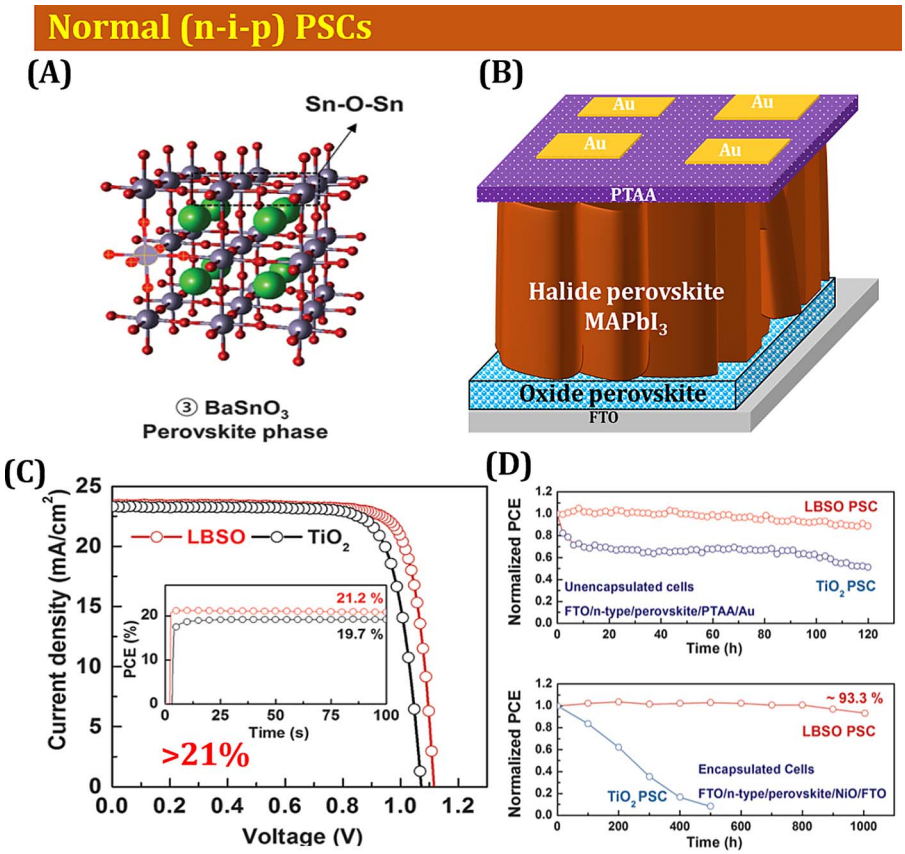


**Figure 1.** (A) Crystal structure of $BaSnO_3$ oxide perovskite phase (B) Schematic of device architecture based on oxide perovskite ETL (C) its photovoltaic performance (D) photostability test after UV radiation. Figs. 1 B, 1C and 1D were reproduced from Ref. 15 with permission from AAAS.

thermal stability. So far, the breakthrough certified efficiency which is based expensive and additives doped spiro-MeOTAD, PTAA and DM HTMs. Furthermore, the precise doping of the TBP, LiTFSI, and FK 209 Co(III) –TFSI salt (FK209) are needed in order to tune the efficiency. For uniform deposition of HTMs, spin coating technique needed which is suffered from high waste of chemical (>90%) which hampers the low-cost production.[21]

After the pioneering work by Mei et al.,[22] many reports discussed the importance of carbon-based HTL towards air and water stability.[23–27] This C-PSCs is also called as HTL-free or printable triple-mesoscopic PSCs. Here, all layers mp-$TiO_2$ and $ZrO_2$ carbon as a HTL were screen-printed. The fabricated fully printable hole-conductor free, mesoscopic triple-layered-based scaffold devices show 12.8% PCE with >1000 hours' ambient air stability. Recently, we have also demonstrated that, the cation degradation can be controlled by providing additional cations from carbon HTL while the compact carbon sealing can improve moisture stability.[28] Furthermore, the bio-inspired method of such "aloe-vera" carbon nanoparticle-based HTL is most convenient, eco-friendly and cheapest one which exhibits >12.5% PCE.[29] Therefore, carbon HTL based PSCs opens a new era toward low-cost and highly stable PSCs. On the same aspect, Ku et al.[30] used carbon counter electrode for fully printable processed mesoscopic perovskite/$TiO_2$ heterojunction solar cells with 6.64% PCE with limit stability due to unstable nature of organic MA cation.

Considering the stability issue of the 3D perovskites, Mohite et al., synthesized 2D Ruddlesden–Popper layered perovskites, $(BA)_2(MA)_2Pb_3I_{10}$ (n = 3) and $(BA)_2(MA)_3Pb_4I_{13}$ (n = 4) (Fig. 2A) {herein $(BA)_2(MA)_{n-1}Pb_nI_{3n+1}$ layered perovskite family}, where $\{(MA)_{n-1}Pb_nI_{3n+1}\}^{2-}$ denotes the anionic layers derived from the parent 3D perovskite, methylammonium lead triiodide ($MAPbI_3$) and deposited by hot-casting technique. The fabricated inverted (p-i-n) devices based on poly(3,4-ethylenedioxythiophene):polystyrene sulfonate (PEDOT:PSS) HTL demonstrated 12.52% PCE. Furthermore, the fabricated un-encapsulated 2D perovskites based devices retain >65% stability over 2250 hours.[31] On the other hand, Gratzel et al. used fully printable C-PSCs (Fig. 2B) and demonstrated 12.9% efficiency with one-year stable performance by engineering an ultra-stable 2D/3D $(HOOC(CH_2)_4NH_3)_2PbI_4/CH_3NH_3PbI_3$ perovskite junction (Fig. 2C).[32,33] Furthermore, in order to up-scale this technique, 10 × 10 $cm^2$ perovskite solar module was fabricated via screen printing technique which exhibited 11.2% PCE with >10,000 hours stable performance retaining 100% stability [Fig. 2D]. Therefore, the HTM free[34–40] or carbon-based HTMs electrodes[41–48] for PSCs are the best option. Similarly, Zhang et al.[49] used $SrCl_2$ based perovskite absorber layer with 16% efficiency. While Wei. et al.,[50] used candle soot technique as a carbon counter electrode with 11.02% (best cell) efficiency. Similarly, bifunctional conjugated organic molecule 4-(aminomethyl) benzoic acid hydroiodide (AB) has been employed as an organic cation in organic–inorganic halide perovskite materials which shows 15.6% PCE[51] for small area and 10% stable PCE for fully printable 10 × 10 $cm^2$ perovskite module.[52] Therefore, development in full printable, low cost, eco-friendly and air-stable HEL for PSCs is urgent need towards commercialization of PSCs at large scale. The carbon-based PSCs (C-PSCs) is one of choice for air-moisture-stable PSCs, but suffered from low efficiency.[53]

***Inorganic low-cost thermally stable HTLs.—***In contrast to their carbon-based HEL counterparts, Jeon et al. tuned the unique composition of 3D perovskite with ratio (0.85:0.15) of $FAPbI_3$:$MAPbBr_3$ exhibited >18% for solvent engineering[54] and 20.5% via vacuum flash solution processed perovskite layer for a bilayer solar-cell architecture.[55] Although, normal n-i-p type showed >23.2% PCE, still preparation of $BaSnO_3$ ETL is complicated and thermal stability was improved by using expensive PTAA or DM HTL. Therefore, implementation of the non-conventional, low-cost, inorganic (i)-HTLs such as CuI[56] $CsSnI_3$[57] and CuSCN[58,59] would be the best choice toward stable PSCs. In case of the highly efficient and thermally stable i-HTL, to date, there is no other option except hexagonal copper(I)

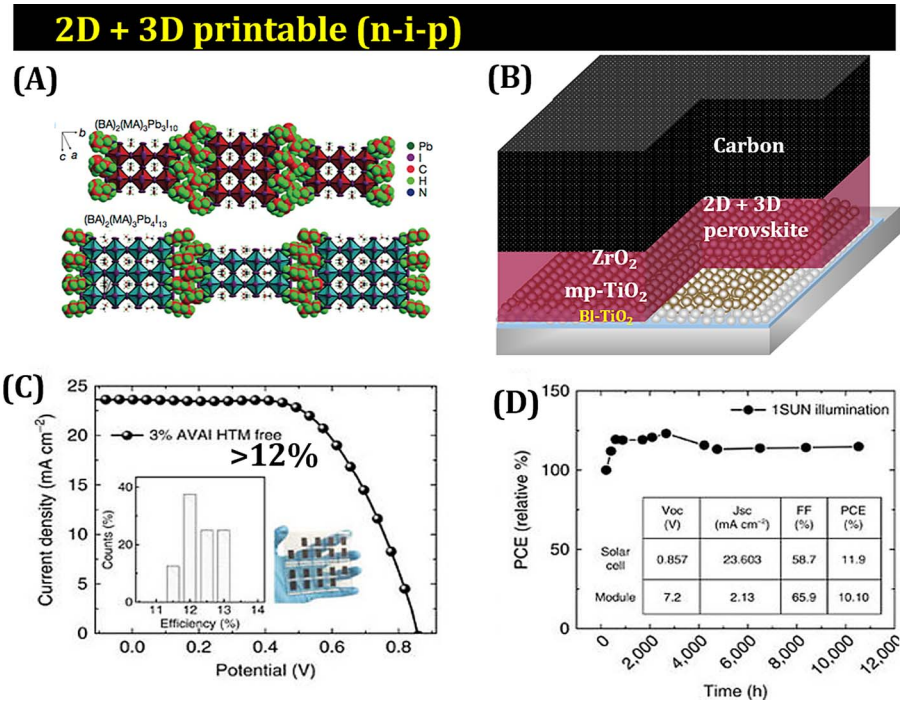


**Figure 2.** (A) The crystal structure of the Ruddlesden–Popper $(BA)_2(MA)_2Pb_3I_{10}$ and $(BA)_2(MA)_3Pb_4I_{13}$ layered perovskites, depicted as n polyhedral blocks, where n refers to the number of layers; the BA spacer layers are depicted as space-fill models to illustrate the termination of the perovskite layers (B) Schematic presentation of fully printable C-PSCs (C) J–V curve using the 2D/3D perovskite with 3% AVAI (device statistics and picture in the inset) (D) Typical module stability ($10 \times 10$ cm$^2$) test under 1 sun AM 1.5 G conditions at stabilized temperature of 55°C and at short circuit conditions. Fig. 2A was reproduced from Ref. 31, with permission Nature Publishing Group, Fig. 2B was reproduced from Ref. 29 with permission American Chemical Society; Figs. 2C and 2D were reproduced from Ref. 32 with permission Nature Publishing Group.

thiocyanate (herein β- CuSCN) (Fig. 3A). Due to its extremely low-cost (< 0.1% of conventional organic HTLs), high thermal stability, high hole-mobility and simple preparation method, CuSCN is most promising i-HTL for highly efficient PSCs with operational stability. Besides, the well-aligned highly occupied molecular orbital (HOMO) level of CuSCN (−5.3 eV) facilitates higher $V_{OC}$. However, due to the unique dissolution of CuSCN in polar diethyl-sulfide solvent is main cause for perovskite layer degradation. Therefore, the use of non-polar solvent coating prior to i-HEL coating is a good idea, but still showed only ∼7% PCE.[60] Seok et al., used mixed halide $(FAPbI_3)_{0.85}(MAPbBr_3)_{0.15}$ and demonstrated 18% PCE.[61] To solve the polar solvent issue, Arora et al. used the dynamic spin-coating technique for CuSCN deposition (Fig. 3B) on highly uniform solvent engineering processed triple-cation based $Cs_{0.05}FA_{0.81}MA_{0.14}PbI_{2.55}Br_{0.45}$ perovskite absorber with ∼19.22 ±0.84% PCE.[62] Furthermore, the implementation of reduced graphene oxide (rGO) interfacial layer between Au metal contact and CuSCN can terminate the metal diffusion revealed >20.4% efficiency ($J_{SC}$ of 23.24 mAcm$^{-2}$, $V_{OC}$ of 1.112 V and FF of 78.2%) with good thermal stability (Fig. 3C). Besides, deposition of ∼2 nm $Al_2O_3$ interfacial spacer layer via atomic layer deposition (ALD) between perovskite and CuSCN layer and poly(methyl methacrylate) (PMMA) coating can extend the thermal stability more than 1000 hours at 60°C (Fig. 3D) with >95% retain its original efficiency.[62] However, deposition of $Al_2O_3$ interfacial spacer layer via

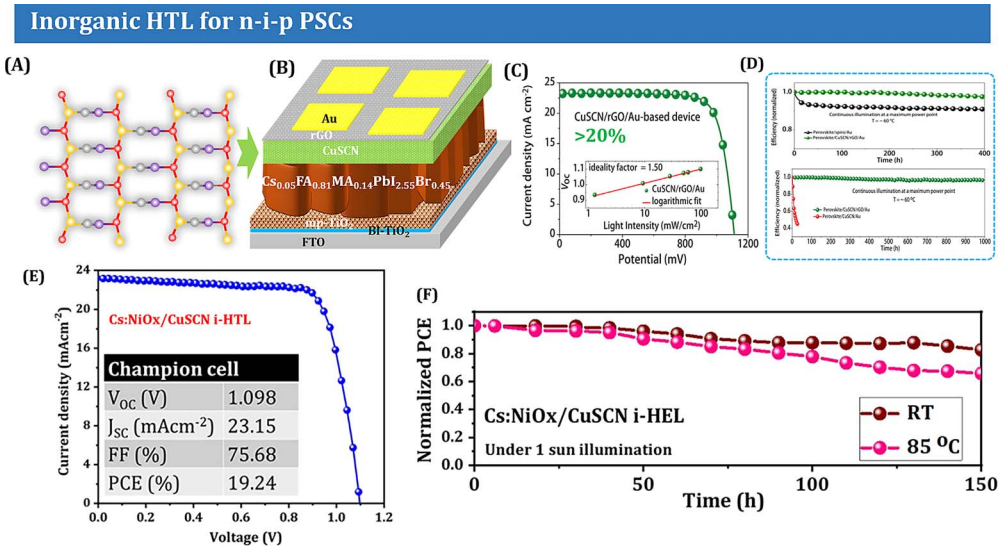


**Figure 3.** (A) The crystal structure of β-CuSCN inorganic HEL (B) Schematic representation of n-i-p type regular PSCs based on CuSCN inorganic HEL. (C) J-V curve respective device; the inset shows the $V_{OC}$ as a function of illumination intensity with an ideality factor of 1.50 (D) Operational stability of un-encapsulated spiro-OMeTAD and CuSCN (top); with and without a thin layer of rGO (as a spacer layer between CuSCN and gold layers) for CuSCN HEL, examined at a maximum power point under continuous full-sun illumination at 60°C in a nitrogen atmosphere. (E) J-V characteristics of Cs:NiOx/CuSCN double i-HEL (F) thermal stability at room temperature and 85°C. Figs. 3C and 3D were reproduced from Ref. 62 with permission from AAAS; Figs. 3E and 3F were reproduced from Ref. 63 with permission Elsevier 2019.

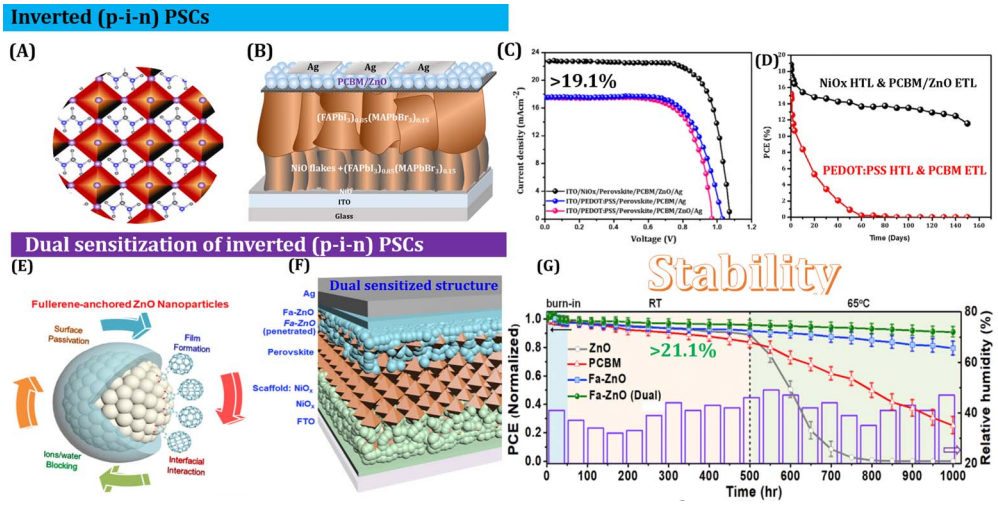


**Figure 4.** (A) Crystal structure 3D $FAPbI_3$ perovskite (B) schematic representation of all metal oxide based inverted (p-i-n) PSCs based on np-NiOx (C) J–V curves of the best performing inverted p-i-n type PSCs based on different HTL and ETLs measured under one sun illumination (100 mW $cm^{-2}$, AM 1.5G). (D) Air-stability of p-i-n type inverted PSCs based on PEDOT:PSS HTL and np-NiOx HTL. (E) Schematic representation of fullerene-anchored ZnO nanoparticles with low surface defects (F) Inverted dual sensitized perovskite device architecture (G) thermal stability with respect to different ETLs. Figs. 4B−4D were reproduced from Ref. 72 with permission Elsevier 2018; Fig. 4E−4G were reproduced from Ref. 73 with permission Elsevier 2018.

ALD is complicated and expensive one. In order to solve polar-solvent issue, Mali et al., deposited Cs:NiOx from chlorobenzene solvent as an active interfacial layer prior to CuSCN deposition acting synergistically to boost efficiency as well as protect perovskite layer from polar solvent. The best efficiency based on Cs:NiOx/CuSCN double-i-HEL devices exhibited 19.24% (Fig. 3E) with >92% thermal stability over 150 h at room temperature and >65% at 85°C under continuous 1 sun illumination (Fig. 3F).[63]

***All metal-oxide ETL, HTL based inverted p-i-n PSCs.—***As per as inverted (p-i-n) type architectures are concern, the perovskite layer is sandwiched between p-type polymers, such as PEDOT:PSS, poly(3-hexylthiophene-2,5-diyl) (P3HT) and n-type fullerene or phenyl-$C_{61}$-butyric acid methyl ester (PCBM) ETL. Recently, Huang et al., developed exfoliated montmorillonite (MMT)/$MAPbI_3$ nanocomposite as photoactive layer and demonstrated 17.29% PCE with half-year stability for p-i-n inverted PSCs.[64] However, this inverted p-i-n type PSCs are suffered from low stability due to diffusion of metal contacts into PCBM/perovskite layer and major hysteresis due to irregular PCBM thickness and poor interfaces. In addition, due to the formation of low energy of lead halide perovskites, acidic nature of PEDOT:PSS organic HTLs and poor-hole mobility, p-i-n PSCs suffer from degradation issue. Therefore, implementation of p-type/n-type metal oxide HTL/ETL (herein all metal oxide PSCs) for p-i-n inverted type PSCs would be the best choice in order to improve the stability and prevent the metal diffusion.[65,66] Furthermore, the pristine and doped p-type metal oxides demonstrate much higher carrier mobility and superior stability as compared to organic materials.[67–69]

So far, various p-type metal oxide HTLs have been used to date for inverted p-i-n PSCs including, $Cu_2O$, CuO, NiOx and Cu:NiOx in order to make stable PSCs. However, due to high hole mobility ($10^{-5}$ to $10^{-3}$ $cm^2$ $V^{-1}$ $s^{-1}$), high air stability and higher $V_{OC}$, pristine and doped NiOx have become a promising HTL for PSCs. In addition, the optimization of delicate interfaces between PCBM (for p-i-n) and top metal electrodes is mandatory in order to improve the stability of PSCs. Therefore, the implementation of ZnO interlayer between PCBM and top metal contacts could terminate the unwanted degradation and diffusion and it protects the perovskite layer from the air. You et al. used solution processed p-type NiOx (HTL) and n-type ZnO (ETL), and showed a 16.1% PCE with 60-days air stability.[70] Chen et al. used stable NiOx as a HTL and poly(2-ethyl-2-oxazoline) (PEOz) nanodots as ETL and demonstrated 18.28% efficiency ($V_{OC}$ = 1.07 V, $J_{SC}$ = 21.93 mA $cm^2$, and FF = 77.9%) with ~800 h an ambient environment stability.[71]

Recently, we synthesized nanoporous nickel oxide (np-NiOx) as an HTL using co-precipitation method having flakes like morphology and stability was maintained by pin-hole free thin PCBM and ZnO ETL by spin coating technique (Fig. 4B).[72] We developed a co-precipitation method in order to synthesize a nanoporous p-type NiOx thin film as a HTL, and $(FAPbI_3)_{0.85}(MAPbBr_3)_{0.15}$ perovskite layer which was protected by PCBM/ZnO nanoparticles as the ETL. The best-performing p-i-n PSC device having np-NiOx HTL, $(FAPbI_3)_{0.85}(MAPbBr_3)_{0.15}$ perovskite and PCBM/ZnO ETL exhibited a 19.10% (±1%) PCE ($J_{SC}$ of 22.76 mA $cm^{-2}$, $V_{OC}$ of 1.076 V and FF of 0.78) under 1 sun (100 $mWcm^{-2}$) (Fig. 4C). Interestingly, the developed p-i-n PSCs based on p-type NiOx and n-type ZnO could retain >80% efficiency after 160 days which is much higher than conventional PEDOT:PSS HTL based PSCs (Fig. 4D). Based on this aspect, recently, Yao et al.,[73] used fullerene-anchored core-shell ZnO nanoparticle (Fa-ZnO) based ETL synthesized by chemical route (Fig. 4E) and mesoporous NiOx used as a HTL for inverted p-i-n device configuration (Fig. 4F). The optimized device exhibited 21.1% PCE with 1000 hours stability at 65°C for dual sensitized perovskite architecture (Fig. 4G). A novel surface-passivation strategy achieved this enhancement was adopted by anchoring ZnO nanoparticles with Fa-ZnO to mitigate trap states and passivate surface hydroxyl groups. Similarly, Seo et al., used $Cs_{0.05}MA_{0.95}PbI_3$ perovskite absorber which is sandwiched between inorganic metal oxide for both HTL and ETL in inverted p-i-n architecture and demonstrated 18.45% PCE with 86.7% retention after 500 hours at 85°C thermal stress.[74] The thermal stability was improved by using ALD deposited Al:ZnO (AZO) and NiOx.

***Toward MA-free perovskites.—***It is well known that the stability of unstable $MAPbI_3$ ($E_g$ = 1.58 eV) can be improved by incorporating $MAPbBr_3$ ($E_g$ = 2.26 eV).[75] However, relatively low-bandgap of black phase (FA) based perovskite $FAPbI_3$ (1.48 eV) with unique composition of $(FAPbI_3)_{0.85}(MAPbBr_3)_{0.15}$ ($E_g$ = 1.54 eV) stabilized at 100°C and pushed PCE 20.8% with $V_{OC}$ up to 1.16 V and $J_{SC}$ of 24.6 $mAcm^{-2}$.[76] The stability of MA-cation is poor than FA-cation. Therefore, implementing a triple/quadrupole (CsI and/or RbI) cations in the above perovskite $(FAPbI_3)_{0.85}(MAPbBr_3)_{0.15}$ composition pushed $V_{OC}$ up to 1.24 V having 1.63 eV bandgap results in 21.6% PCE with better stability via PTAA HTM.[18] Jung et al., used butylammonium (BA) and phenethylammonium (PEA) cations modified $MAPbI_3$ perovskite and

demonstrated 20.1% PCE with >760 hours stability at 80°C. However, cost and additives doping issue remained.[77] Recently, MA-free perovskite absorber $Rb_5Cs_{10}FAPbI_3$ demonstrated 18.16% PCE after 1000 hours at 85°C.[78] However, the preparation of AZO and NiOx by ALD is expensive. Therefore, an alternative method need to develop for deposition of these HTLs and ETLs.

## Future Needs and Prospects

Thinking out-of-the-box, the implementation of low-cost thermal-stable i-HEL (either carbon, CuSCN or metal oxide HTL) and doped oxide perovskites ETL and HTL with reduced and/or MA-cation free composition of environmentally stable 2D/3D perovskites with single junction or tandem cell could be a potential impact toward highly efficient, thermally-stable, low-cost industrial scale device fabrication. So far, more attention has been paid to the development of MA or FA cation based perovskite absorber layer, including lead-free composition. However, the critical issue is poor stability of the MA-cation and precise additives doping in conditional HTMs. Therefore, the promising approach is to develop a MA-reduced or MA-cation free perovskite absorber with additives dopant-free HTM. Although, fully-printable C-PSCs shows much simplistic approach toward commercialization but still suffered from high efficiency. Besides, Si-Perovskite tandem solar cell shows >25.2% PCE, however, the optimization of each layer is a difficult task. Therefore, there are four main challenges in the PSCs technology as follows:

Challenges for perovskite photovoltaics:

a. Maintain the self-degradation of perovskite layer to achieve long-term stability.
b. Efforts should be made on more efficient compositions which covers solar spectrum effectively.
c. Upscaling from lab-scale to industrial scale without compromising its losses.
d. Outdoor operational stability at module scale.

## Conclusions

In conclusion, we believe that, the solution-processed inorganic ETLs as well as HTLs and modified organic cations and/or organic cation free perovskite absorber layers such as BA-MA or PEA-MA,[77] $RbFAPbI_3$,[78] $CsPbI_2Br$, $CsPb_{0.95}Eu_{0.05}I_2Br$[79] would be the best choice toward air-thermal-moisture stable PSCs. Besides these, the uniform deposition of HTL and ETL and formation of textured perovskite absorber layer over large scale via conventional deposition technique is still a big challenge. Therefore, further investigation on the alternative deposition techniques such as ultrasonic-spray,[80,81] roll-to-roll (R2R),[82] doctor-blade,[83,84] slot-die,[85–87] solvent- and vacuum-free route,[88] meniscus-assisted solution printing[89] and air bladding,[90,91] process are needed to apply for further development in order to commercialize the PSCs product. Achieving highly stable PSCs could develop low-cost photovoltaic technology by paving the way for more cost-effective photovoltaic technology. We believing that, this methodology can contribute a significant breakthrough toward commercialization of stable perovskite photovoltaics with >25%† efficiency over 5 × 5 $cm^2$ area.

## Acknowledgments

This research was supported by the National Research Foundation of Korea (NRF) (NRF-2017R1A2B4008117). This work was also supported by the Korea Research Fellowship Program through the National Research Foundation of Korea (NRF) funded by the Ministry of Science, ICT and Future Planning (2016H1D3A1909289) for an outstanding overseas young researcher. This work was supported by Priority Research Centers Program through the National Research Foundation of Korea (NRF) funded by the Ministry of Education, Science and Technology (2018R1A6A1A03024334). This work was also supported by a National Research Foundation of Korea (NRF) grant funded by the Korea government (MSIT) (2018R1C1B6008218).

## ORCID

Sawanta S. Mali https://orcid.org/0000-0002-4973-4203

## References

1. C. Battaglia, A. Cuevas, and S. De Wolf, "High-efficiency crystalline silicon solar cells: status and perspectives." *Energy Environ. Sci.*, **9**, 1552 (2016).
2. A. Richter, M. Hermle, and S. Glunz, "Crystalline silicon solar cells reassessment of the limiting efficiency for crystalline silicon solar cells." *IEEE J. Photovolt.*, **3**, 1184 (2013).
3. K. Yoshikawa, H. Kawasaki, W. Yoshida, T. Irie, K. Konishi, K. Nakano, T. Uto, D. Adachi, M. Kanematsu, and H. Uzu, "Silicon Heterojunction Solar Cell with Interdigitated Back Contacts for a Photoconversion Efficiency over 26%." *Nat. Energy*, **2**, 17032 (2017).
4. S. Essig et al. "Raising the one-sun conversion efficiency of III–V/Si solar cells to 32.8% for two junctions and 35.9% for three junctions." *Nat. Energy*, **2**, 17144 (2017).
5. Oxford PV Retrieved from https://www.oxfordpv.com/news/oxford-pv-sets-world-record-perovskite-solar-cell (25 June 2018).
6. F. Sahli, J. Werner, B. A. Kamino, M. Brauninger, R. Monnard, B. Paviet-Salomon, L. Barraud, L. Ding, J. J. Diaz Leon, D. Sacchetto et al. "Fully Textured Monolithic Perovskite/Silicon Tandem Solar Cells With 25.2% Power Conversion Efficiency." *Nat. Mater.*, **17**, 820 (2018).
7. W. Shockley and H. J. Queisser, *J. Appl. Phys.*, **32**, 510 (1961).
8. W. E. I. Sha, X. Ren, L. Chen, and W. C. H. Choy, *Appl. Phys. Let*, **106**, 221104 (2015).
9. X. Zeng, T. Zhou, C. Leng, Z. Zang, M. Wang, W. Hu, X. Tang, S. Lu, L. Fang, and M. Zhou, "Performance Improvement of Perovskite Solar Cell by Employing CdSe Quantum Dot/PCBM Composite as Electron Transport Layer," *J. Mater. Chem. A*, **5**, 17499 (2017).
10. B. Yang, M. Wang, X. Hu, T. Zhou, and Z. Zang, "Highly Efficient Semitransparent $CsPbIBr_2$ Perovskite Solar Cells via Low-temperature Processed $In_2S_3$ as Electron-transport-layer," *Nano Energy*, **57**, 718 (2019).
11. M. Wang, Z. Zang, B. Yang, X. Hu, K. Sun, and L. Sun, "Performance improvement of perovskite solar cells through enhanced hole extraction: The role of iodide concentration gradient," *Sol. Energy Mater. Sol. Cells*, **185**, 117 (2018).
12. T. Zhou, M. Wang, Z. Zang, X. Tang, and L. Fang, "Two-dimensional lead-free hybrid halide perovskite using superatom anions with tunable electronic properties," *Solar Energy Mater. Sol. Cells*, **191**, 33 (2019).
13. S. S. Mali and C. K. Hong, "p-i-n/n-i-p type planar hybrid structure of highly efficient perovskite solar cells toward improved air stability: synthetic strategies and the role of p-type hole transport layer (HTL) and n-type electron transport layer (ETL) metal oxides," *Nanoscale*, **8**, 10528 (2016).
14. N. J. Jeon, H. Na, E. H. Jung, T.-Y Yang, Y. G. Lee, G. Kim, H.-W. Shin, S. I. Seok, J. Lee, and J. Seo, "A fluorene-terminated hole-transporting material for highly efficient and stable perovskite solar cells," *Nature Energy*, **3**, 682 (2018).
15. S. S. Shin, E. J. Yeom, W. S. Yang, S. Hur, M. G. Kim, J. Im, J. Seo, J. H. Noh, and S. I. Seok, "Colloidally prepared La-doped $BaSnO_3$ electrodes for efficient, photostable perovskite solar cells," *Science*, **356**, 167 (2017).
16. A. Kojima, K. Teshim, Y. Shirai, and T. Miyasaka, "Organometal Halide Perovskites as Visible-Light Sensitizers for Photovoltaic Cells," *J. Am. Chem. Soc.*, **131**, 6050 (2009).
17. J.-H. Im, C. R. Lee, J. W. Lee, S. W. Park, and N. G. Park, "6.5% efficient perovskite quantum-dot-sensitized solar cell," *Nanoscale*, **3**, 4088 (2011).
18. W. S. Yang, B.-W. Park, E. H. Jung, N. J. Jeon, Y. C. Kim, D. U. Lee, S. S. Shin, J. Seo, E. K. Kim, J. H. Noh, and S. I. Seok, "Iodide management in formamidinium-lead-halide–based perovskite layers for efficient solar cells," *Science*, **356**, 1376 (2017).
19. M. Saliba, T. Matsui, K. Domanski, J.-Y. Seo, A. Ummadisingu, S. M. Zakeeruddin, J.-P. Correa-Baena, W. Tress, A. Abate, A. Hagfeldt, and M. Grätzel, "Incorporation of rubidium cations into perovskite solar cells improves photovoltaic performance," *Science*, **354**, 206 (2016).
20. H. Tan, A. Jain, O. Voznyy, X. Lan, F. P. G. de Arquer, J. Z. Fan, R. Quintero-Bermudez, M. Yuan, B. Zhang, Y. Zhao, F. Fan, P. Li, L. N. Quan, Y. Zhao, Z.-H. Lu, Z. Yang, S. Hoogland, and E. H. Sargent, "Efficient and stable solution-processed planar perovskite solar cells via contact passivation," *Science*, **355**, 722 (2017).
21. M. Remeika and Y. Qi, "Scalable solution coating of the absorber for perovskite solar cells," *J. Energy Chem.*, **27**, 1101 (2017).
22. A. Mei, X. Li, L. Liu, Z. Ku, T. Liu, Y. Rong, M. Xu, M. Hu, J. Chen, Y. Yang, M. Gratzel, and H. Han, "A hole-conductor–free, fully printable mesoscopic perovskite solar cell with high stability," *Science*, **345**, 295 (2014).
23. H. Chen and S. Yang, "Stabilizing and scaling up carbon-based perovskite solar cells," *J. Mater. Res.*, **32**, 3011 (2017).
24. Y. Liu, S. Ji, S. Li, W. He, K. Wang, H. Hu, and C. Ye, "Study on hole-transport-material-free planar $TiO_2/CH_3NH_3PbI_3$ heterojunction solar cells: the simplest configuration of a working perovskite solar cell," *J. Mat. Chem. A*, **3**, 14902 (2015).
25. W. A. Labana and L. Etgar, "Depleted hole conductor-free lead halide iodide heterojunction solar cells," *Energy Environ. Sci.*, **6**, 3249 (2013).

26. Y. Sheng, Y. Hu, A. Mei, P. Jiang, X. Hou, M. Duan, L. Hong, Y. Guan, Y. Rong, Y. Xiong, and H. Han, "Enhanced electronic properties in $CH_3NH_3PbI_3$ via LiCl mixing for hole-conductor-free printable perovskite solar cells," *J. Mater. Chem. A*, **4**, 16731 (2016).
27. C. Y. Chan, Y. Y. Wang, G. W. Wu, and E. W. G. Diau, "Solvent-extraction crystal growth for highly efficient carbon-based mesoscopic perovskite solar cells free of hole conductors," *J. Mater. Chem. A*, **4**, 3872 (2016).
28. S. S. Mali, H. J. Kim, H. H. Kim, G. R. Park, S. E. Shim, and C. K. Hong, "Large area, waterproof, air stable and cost effective efficient perovskite solar cells through modified carbon hole extraction layer," *Mater. Today Chem.*, **4**, 53 (2017).
29. S. S. Mali, H. J. Kim, J. V. Patil, and C. K. Hong, "Bio-inspired Carbon Hole Transporting Layer Derived from Aloe Vera Plant for Cost-Effective Fully Printable Mesoscopic Carbon Perovskite Solar Cells," *ACS Appl. Mater. Interfaces*, **10**, 31280 (2018).
30. Z. Ku, Y. Rong, M. Xu, T. Liu, and H. Han, "Full Printable Processed Mesoscopic $CH_3NH_3PbI_3/TiO_2$ Heterojunction Solar Cells with Carbon Counter Electrode," *Sci. Rep.*, **3**, 3132 (2013).
31. H. Tsai, W. Nie, J.-C. Blancon, C. C. Stoumpos, R. Asadpour, B. Harutyunyan, A. J. Neukirch, R. Verduzco, J. J. Crochet, S. Tretiak, L. Pedesseau, J. Even, M. A. Alam, G. Gupta, J. Lou, P. M. Ajayan, M. J. Bedzyk, M. G. Kanatzidis, and A. D. Mohite, "High-efficiency two-dimensional Ruddlesden-Popper perovskite solar cells." *Nature*, **536**, 312 (2016).
32. G. Grancini, C. Roldán-Carmona, I. Zimmermann, E. Mosconi, X. Lee, D. Martineau, S. Narbey, F. Oswald, F. De Angelis, M. Graetzel, and M. K. Nazeeruddin, "One-Year stable perovskite solar cells by 2D/3D interface engineering," *Nat. Comm.*, **8**, 15684 (2017).
33. S. G. Hashmi, D. Martineau, M. Ibrahim Dar, T. T. T. Myllymäki, T. Sarikka, V. Ulla, S. M. Zakeeruddin, and M. Grätzel, "High performance carbon-based printed perovskite solar cells with humidity assisted thermal treatment," *J. Mater. Chem. A*, **5**, 12060 (2017).
34. M. Hambsch, Q. Lin, A. Armin, P. L. Burn, and P. Meredith, "Efficient, monolithic large area organohalide perovskite solar cells," *J. Mater. Chem. A*, **4**, 13830 (2016).
35. Y. Yang, J. Xiao, H. Wei, L. Zhu, D. Li, Y. Luo, H. Wu, and Q. Meng, "An all-carbon counter electrode for highly efficient hole-conductor-free organo-metal perovskite solar cells," *RSC Adv.* **4**, 52825 (2014).
36. Z. Wei, H. Chen, K. Yan, and S. Yang, "Inkjet printing and instant chemical transformation of a $CH_3NH_3PbI_3$/nanocarbon electrode and interface for planar perovskite solar cells," *Angew. Chem.*, **53**, 13239 (2014).
37. H. Chen and S. Yang, "High-quality perovskite in thick scaffold: a core issue for hole transport material-free perovskite solar cell," *Sci. Bull.*, **61**, 1680 (2016).
38. A. K. Baranwal, S. Kanaya, T. A. Nirmal Peiris, G. Mizuta, T. Nishina, H. Kanda, T. Miyasaka, H. Segawa, and S. Ito, "100 °C Thermal Stability of Printable Perovskite Solar Cells Using Porous Carbon Counter Electrodes," *ChemSusChem*, **9**, 2604 (2016).
39. F. Zhang, X. Yang, H. Wang, M. Cheng, J. Zhao, and L. Sun, "Structure Engineering of Hole–Conductor Free Perovskite-Based Solar Cells with Low-Temperature-Processed Commercial Carbon Paste As Cathode," *ACS Appl. Mater. Interfaces*, **6**, 16140 (2014).
40. H. Zhou, Y. Shi, Q. Dong, Zhang H, Y. Xing, K. Wang, Y. Du, and T. Ma, "Hole-Conductor-Free, Metal-Electrode-Free $TiO_2/CH_3NH_3PbI_3$ Heterojunction Solar Cells Based on a Low-Temperature Carbon Electrode," *J. Phys. Chem. Lett.*, **5**, 3241 (2014).
41. W. Peng et al., "Solution-Grown Monocrystalline Hybrid Perovskite Films for Hole-Transporter-Free Solar Cells," *Adv. Mat.*, **28**, 3383 (2016).
42. S. Gholipour, J. P. Correa-Baena, K. Domanski, T. Matsui, L. Steier, F. Giordano, F. Tajabadi, W. Tress, M. Saliba, A. Abate, A. M. Ali, N. Taghavinia, M. Grätzel, and A. Hagfeldt, "Highly Efficient and Stable Perovskite Solar Cells based on a Low-Cost Carbon Cloth," *Adv. Energy Mater*, **6**, 1601116 (2016).
43. S. Collavini and J. L. Delgado, "Carbon Nanoforms in Perovskite-Based Solar Cells," *Adv. Energy Mater*, **7**, 1601000 (2017).
44. H. Chen, Z. Wei, H. He, X. Zheng, K. S. Wong, and S. Yang, "Solvent Engineering Boosts the Efficiency of Paintable Carbon-Based Perovskite Solar Cells to Beyond 14%," *Adv. Energy Mat.*, **6**, 1502087(2016).
45. W. Wei and Y. H. Hu, "Highly conductive Na-embedded carbon nanowalls for hole-transport-material-free perovskite solar cells without metal electrodes," *J. Mater. Chem. A*, **5**, 24126 (2017).
46. H. Chen, X. Zheng, Q. Li, Y. Yang, S. Xiao, C. Hu, Y. Bai, T. Zhang, K. Sing Wong, and S. Yang, "An amorphous precursor route to the conformable oriented crystallization of $CH_3NH_3PbBr_3$ in mesoporous scaffolds: toward efficient and thermally stable carbon-based perovskite solar cells," *J. Mat. Chem. A*, **4**, 12897 (2016).
47. L. Liu, A. Mei, T. Liu, P. Jiang, Y. Sheng, L. Zhang, and H. Han, "Fully Printable Mesoscopic Perovskite Solar Cells with Organic Silane Self-Assembled Monolayer," *J. Am. Chem. Soc.*, **137**, 1790 (2015).
48. H. Chen, Z. Wei, X. Zheng, and S. Yang, "A scalable electrodeposition route to the low-cost, versatile and controllable fabrication of perovskite solar cells," *Nano Energy*, **15**, 216 (2015).
49. H. Zhang, H. Wang, S. T. Williams, D. Xiong, W. Zhang, C. C. Chueh, W. Chen, and A. K.-Y. Jen, "$SrCl_2$ Derived Perovskite Facilitating a High Efficiency of 16% in Hole-Conductor-Free Fully Printable Mesoscopic Perovskite Solar Cells," *Adv. Mater.*, **29**, 1606608 (2017).
50. Z. Wei, K. Yan, H. Chen, Y. Yi, T. Zhang, X. Long, J. Li, L. Zhang, J. Wang, and S. Yang, "Cost-efficient clamping solar cells using candle soot for hole extraction from ambipolar perovskites," *Energy Environ. Sci.*, **7**, 3326 (2014).
51. Y. Hu, Z. Zhang, A. Mei, Y. Jiang, X. Hou, Q. Wang, K. Du, Y. Rong, Zhou Y, G. Xu, and H. Han, "Improved Performance of Printable Perovskite Solar Cells with Bifunctional Conjugated Organic Molecule," *Adv. Mater.*, **30**, 1705786 (2018).
52. Y. Hu, S. Si, A. Mei, Y. Rong, H. Liu, X. Li, and H. Han, "Stable Large-Area ($10 \times 10\,cm^2$) Printable Mesoscopic Perovskite Module Exceeding 10% Efficiency," *Solar RRL*, **1**, 1600019 (2017).
53. Y. Yang, H. Chen, X. Zheng, X. Meng, T. Zhang, C. Hu, Y. Bai, S. Xiao, and S. Yang, "Ultrasound-spray deposition of multi-walled carbon nanotubes on NiO nanoparticles-embedded perovskite layers for high-performance carbon-based perovskite solar cells," *Nano Energy*, **42**, 322 (2017).
54. N. J. Jeon, J. H. Noh, W. S. Yang, Y. C. Kim, S. Ryu, J. Seo, and S. I. Seok, "Compositional engineering of perovskite materials for high-performance solar cells," *Nature*, **517**, 476 (2015).
55. X. Li, D. Bi, C. Yi, J.-D. Décoppet, J. Luo, S. M. Zakeeruddin, A. Hagfeldt, and M. Grätzel, "A vacuum flash-assisted solution process for high-efficiency large-area perovskite solar cells," *Science*, **353**, 58 (2016).
56. J. A. Christians, R. C. M. Fung, and P. V. Kamat, "An Inorganic Hole Conductor for Organo-Lead Halide Perovskite Solar Cells. Improved Hole Conductivity with Copper Iodide," *J. Am. Chem. Soc.*, **136**, 758 (2014).
57. I. Chung, B. Lee, J. He, R. P. H. Chang, and M. G. Kanatzidis, "All-solid-state dye-sensitized solar cells with high efficiency," *Nature*, **485**, 486 (2012).
58. P. Qin, S. Tanaka, S. Ito, N. Tetreault, K. Manabe, H. Nishino, M. K. Nazeeruddin, and M. Grätzel, "Inorganic hole conductor-based lead halide perovskite solar cells with 12.4% conversion efficiency," *Nat. Commun.*, **5**, 3834 (2014).
59. V. E. Madhavan, I. Zimmermann, C. Roldán-Carmona, G. Grancini, M. Buffiere, A. Belaidi, and M. Khaja Nazeeruddin, "Copper Thiocyanate Inorganic Hole-Transporting Material for High-Efficiency Perovskite Solar Cells," *ACS Energy Lett.* **1**, 1112 (2016).
60. G. A. Sepalage, S. Meyer, A. R. Pascoe, A. D. Scully, U. Bach, Y.-B. Cheng, and L. Spiccia, "A facile deposition method for CuSCN: Exploring the influence of CuSCN on J-V hysteresis in planar perovskite solar cells," *Nano Energy*, **32**, 310 (2017).
61. M. Jung, Y. C. Kim, N. J. Jeon, W. S. Yang, J. Seo, J. H. Noh, and S. I. Seok, "Thermal Stability of CuSCN Hole Conductor-Based Perovskite Solar Cells," *ChemSusChem*, **9**, 2592 (2016).
62. N. Arora, M. I. Dar, A. Hinderhofer, N. Pellet, F. Schreiber, S. M. Zakeeruddin, and M. Grätzel, "Perovskite solar cells with CuSCN hole extraction layers yield stabilized efficiencies greater than 20," *Science*, **358**, 768 (2017).
63. S. S. Mali, J. V. Patil, H. J. Kim, R. Luque, and C. K. Hong, "Highly efficient thermally stable perovskite solar cells via Cs:NiOx/CuSCN double-inorganic hole extraction layer interface engineering," *Mater. Today*, 2019 (in press).
64. H. H. Huang, Y. C. Shih, L. Wang, and K. F. Lin, "Boosting the ultra-stable unencapsulated perovskite solar cells by using montmorillonite/$CH_3NH_3PbI_3$ nanocomposite as photoactive layer," *Energy Environ. Sci.*, **12**, 1265 (2019).
65. S. Bai, Z. Wu X. Wu, Y. Jin, N. Zhao, Z. Chen, Q. Mei, X. Wang, Z. Ye, T. Song, R. Liu, S. Lee, and B. Sun, "High-performance planar heterojunction perovskite solar cells: Preserving long charge carrier diffusion lengths and interfacial engineering," *Nano Res.* **7**, 1749 (2014).
66. W. Chen, Y. Wu, J. Liu, C. Qin, X. Yang, A. Islam, Y.-B. Cheng, and L. Han, "Hybrid interfacial layer leads to solid performance improvement of inverted perovskite solar cells," *Energy Environ. Sci.*, **8**, 629 (2015).
67. H. Zhang, H. Wang, W. Chen, and A. K.-Y. Jen, "$CuGaO_2$: A Promising Inorganic Hole-Transporting Material for Highly Efficient and Stable Perovskite Solar Cells," *Adv. Mater.*, **29**, 1604984 (2017).
68. J.-Y. Jeng, K. C. Chen, T. Y. Chiang, P. Y. Lin, T. D. Tsai, Y. C. Chang, T. F. Guo, P. Chen, T. C. Wen, and Y. J. Hsu, "Nickel Oxide Electrode Interlayer in $CH_3NH_3PbI_3$ Perovskite/PCBM Planar-Heterojunction Hybrid Solar Cells," *Adv. Mater.*, **26**, 4107 (2014).
69. X. Yin, P. Chen, M. Que, Y. Xing, W. Que, C. Niu, and J. Shao, "Highly Efficient Flexible Perovskite Solar Cells Using Solution-Derived $NiO_x$ Hole Contacts," *ACS Nano*, **10**, 3630 (2016).
70. J. You, L. Meng, T. B. Song, T. F. Guo, Y. Michael Yang, W. H. Chang, Z. Hong, H. Chen, H. Zhou, Q. Chen, Y. Liu, N. D. Marco, and Y. Yang, "Improved air stability of perovskite solar cells via solution-processed metal oxide transport layers," *Nat. Nanotechnol.*, **11**, 75 (2016).
71. W. Chen, G. Zhanga, L. Xu, R. Gu, Z. Xu, H. Wang, and Z. He, "Low temperature processed, high-performance and stable NiOx based inverted planar perovskite solar cells via a poly(2-ethyl-2-oxazoline) nanodots cathode electron-extraction layer," *Mater. Today Energy*, **1–2**, 1 (2016).
72. S. S. Mali, H. J. Kim, H. H. Kim, C. E. Shim, and C. K. Hong, "Nanoporous p-type NiOx electrode for p-i-n inverted perovskite solar cell toward air stability," *Mater. Today*, **21**, 483 (2018).
73. K. Yao, S. Leng, Z. Liu, L. Fei, Y. Chen, S. Li, N. Zhou, J. Zhang, Y. X. Xu, L. Zhou, H. Huang, and A. K.-Y. Jen, "Fullerene-Anchored Core-Shell ZnO Nanoparticles for Efficient and Stable Dual-Sensitized Perovskite Solar Cells," *Joule*, **3**, 417 (2019).
74. S. Seo, S. Jeong, C. Bae, N. G. Park, and H. Shin, "Perovskite Solar Cells with Inorganic Electron- and Hole-Transport Layers Exhibiting Long-Term (≈500h) Stability at 85°C under Continuous 1 Sun Illumination in Ambient Air," *Adv. Mater.*, **30**, 1801010 (2018).
75. J. H. Noh, S. H. Im, J. H. Heo, T. N. Mandal, and S. I. Seok, "Chemical Management for Colorful, Efficient, and Stable Inorganic–Organic Hybrid Nanostructured Solar Cells," *Nano Lett.*, **13**, 1764 (2013).
76. W. S. Yang, J. H. Noh, N. J. Jeon, Y. C. Kim, S. Ryu, J. Seo, and S. I. Seok, "High-performance photovoltaic perovskite layers fabricated through intramolecular exchange," *Science*, **348**, 1234 (2015).
77. M. Jung, T. J. Shin, J. Seo, G. Kim, and S. I. Seok, "Structural features and their functions in surfactantarmoured methylammonium lead iodide perovskites for highly efficient and stable solar cells," *Energy Environ. Sci.*, **11**, 2188 (2018).
78. S. H. Turren-Cruz, A. Hagfeldt, and M. Saliba, "Methylammonium-free, high-

performance and stable perovskite solar cells on a planar architecture," *Science*, **362**, 449 (2018).
79. W. Xiang et al., "Europium-Doped $CsPbI_2Br$ for Stable and Highly Efficient Inorganic Perovskite Solar Cells," *Joule*, **3**, 205 (2019).
80. S. Das, B. Yang, G. Gu, P. C. Joshi, I. N. Ivanov, C. M. Rouleau, T. Aytug, D. B. Geohegan, and K. Xiao, "High-Performance Flexible Perovskite Solar Cells by Using a Combination of Ultrasonic Spray-Coating and Low Thermal Budget Photonic Curing," *ACS Photonics*, **2**, 680 (2015).
81. M. Habibi, A. Rahimzadeh, I. Bennouna, and M. Eslamian, "Defect-free large-area (25 $cm^2$) light absorbing perovskite thin films made by spray coating," *Coatings*, **7**, 42 (2017).
82. Q. Hu, H. Wu, J. Sun, D. Yan, Y. Gao, and J. Yang, "Large-area perovskite nanowire arrays fabricated by large-scale roll-to-roll micro-gravure printing and doctor blading," *Nanoscale*, **8**, 5350 (2016).
83. Y. H. Deng, E. Peng, Y. C. Shao, Z. G. Xiao, Q. F. Dong, and J. S. Huang, "Scalable fabrication of efficient organolead trihalide perovskite solar cells with doctor-bladed active layers," *Energy Environ. Sci*, **8**, 1544 (2015).
84. M. Yang, Z. Li, M. O. Reese, O. G. Reid, D. H. Kim, S. Siol, T. R. Klein, Y. Yan, J. J. Berry, M. F. A. M. van Hest, and K. Zhu, "Perovskite ink with wide processing window for scalable high-efficiency solar cells." *Nat. Energy*, **2**, 17038 (2017).
85. J. B. Whitaker, D. H. Kim, B. W. Larson, F. Zhang, J. J. Berry, M. F. A. M. van Hest, and K. Zhu, "Scalable slot-die coating of high performance perovskite solar cells," *Sustainable Energy Fuels*, **2**, 2442 (2018).
86. K. Hwang, Y. S. Jung, Y. J. Heo, F. H. Scholes, S. E. Watkins, J. Subbiah, D. J. Jones, D. Y. Kim, and D. Vak, "Toward large scale roll-to-roll production of fully printed perovskite solar cells," *Adv Mater*, **27**, 1241 (2015).
87. T. Qin W. Huangc, J.-E. Kim, D. Vak, C. Forsythd, C. R. McNeillc, and Y.-B. Chengc, "Amorphous hole-transporting layer in slot-die coated perovskite solar cells," *Nano Energy*, **31**, 210 (2017).
88. H. Chen, F. Ye, W. Tang, J. He, M. Yin, Y. Wang, F. Xie, E. Bi, X. Yang, M. Grätzel, and L. Han, "A solvent- and vacuum-free route to large-area perovskite films for efficient solar modules," *Nature*, **550**, 92 (2017).
89. M. He, B. Li, X. Cui, B. Jiang, Y. He, Y. Chen, D. O'Neil, P. Szymanski, M. A. EI-Sayed, J. Huang, and Z. Lin, "Meniscus-assisted solution printing of large-grained perovskite films for high-efficiency solar cells," *Nat. Commun.*, **8**, 16045 (2017).
90. L. Gao, C. X. Li, C. J. Li, and G. J. Yang, "Large-area high-efficiency perovskite solar cells based on perovskite films dried by the multi-flow air knife method in air," *J. Mater. Chem. A*, **5**, 1548 (2017).
91. J. Ding, Q. Han, Q.-Q. Ge, D.-J. Xue, J.-Y. Ma, B.-Y. Zhao, Y.-X. Chen, J. Liu, D. B. Mitzi, and J.-S. Hu, "Fully Air-Bladed High-Efficiency Perovskite Photovoltaics," *Joule*, **3**(2), 402 (2019).